Characterization of the dehydrogenase-reductase DHRS2 and its involvement in histone deacetylase inhibition in urological malignancies

Melanie R. Müller, Aaron Burmeister, Margaretha A. Skowron, Alexa Stephan, Christian Söhngen, Philipp Wollnitzke, Patrick Petzsch, Leandro A. Alves Avelar, Thomas Kurz, Karl Köhrer, Bodo Levkau, Daniel Netersheim

Article - Version of Record

Experimental Cell Research 439 (2024) 114055

Contents lists available at ScienceDirect

Experimental Cell Research

journal homepage: www.elsevier.com/locate/yexcr

Research article

Characterization of the dehydrogenase-reductase DHRS2 and its involvement in histone deacetylase inhibition in urological malignancies

Melanie R. Müller [a,b,1], Aaron Burmeister [a,b,1], Margaretha A. Skowron [a,b,1], Alexa Stephan [a,b], Christian Söhngen [a,b], Philipp Wollnitzke [c], Patrick Petzsch [d], Leandro A. Alves Avelar [e], Thomas Kurz [e], Karl Köhrer [d], Bodo Levkau [c], Daniel Nettersheim [a,b,*]

[a] Department of Urology, Urological Research Laboratory, Translational UroOncology, Medical Faculty and University Hospital Düsseldorf, Heinrich Heine University Düsseldorf, Germany
[b] Center for Integrated Oncology Aachen Bonn Cologne Düsseldorf (CIO ABCD), Düsseldorf, Germany
[c] Institute of Molecular Medicine III, University Hospital Düsseldorf, Heinrich Heine University Düsseldorf, Germany
[d] Genomics and Transcriptomics Laboratory (GTL), Biological and Medical Research Center (BMFZ), Medical Faculty and University Hospital Düsseldorf, Heinrich Heine University, Germany
[e] Department of Pharmaceutical and Medical Chemistry, Heinrich Heine University Düsseldorf, Düsseldorf, Germany

ARTICLE INFO

Keywords:
DHRS2
Histone deacetylase inhibitor
Germ cell tumors
Urothelial cancer
Prostate cancer
Renal cell carcinoma
Lipid metabolism
Energy metabolism

ABSTRACT

Background: Being implicated during tumor migration, invasion, clonogenicity, and proliferation, the nicotinamide adenine dinucleotide (NAD)/-phosphate (NADP)-dependent dehydrogenase/reductase member 2 (DHRS2) has been considered to be induced upon inhibition of histone deacetylases (HDACi). In this study, we evaluated the current knowledge on the underlying mechanisms of the (epi)genetic regulation of *DHRS2*, as well as its function during tumor progression.

Methods: DHRS2 expression was evaluated on mRNA- and protein-level upon treatment with HDACi by means of qRT-PCR and western blot analyses, respectively. Re-analysis of RNA-sequencing data gained insight into expression of specific *DHRS2* isoforms, while re-analysis of ATAC-sequencing data shed light on the chromatin accessibility at the *DHRS2* locus. Further examination of the energy and lipid metabolism of HDACi-treated urologic tumor cells was performed using liquid chromatography-mass spectrometry.

Results: Enhanced *DHRS2* expression levels upon HDACi treatment were directly linked to an enhanced chromatin accessibility at the *DHRS2* locus. Particularly the *DHRS2 ENST00000250383.11* protein-coding isoform was increased upon HDACi treatment. Application of the HDACi quisinostat only mildly influenced the energy metabolism of urologic tumor cells, though, the analysis of the lipid metabolism showed diminished sphingosine levels, as well as decreased S1P levels. Also the ratios of S1P/sphingosine and S1P/ceramides were reduced in all four quisinostat-treated urologic tumor cells.

Conclusions: With the emphasis on urologic malignancies (testicular germ cell tumors, urothelial, prostate, and renal cell carcinoma), this study concluded that elevated DHRS2 levels are indicative of a successful HDACi treatment and, thereby offering a novel putative predictive biomarker.

1. Background

The dehydrogenase/reductase member 2 (DHRS2), previously known as Hep27 due to its isolation from HepG2 hepatocellular carcinoma cells by Donadel et al., in 1991 [1], is a member of the nicotinamide adenine dinucleotide (NAD)/-phosphate (NADP)-dependent short-chain dehydrogenase/reductase (SDR) protein family [2,3]. Located on chromosome 14q11.2, a region frequently deleted in different tumor entities, *DHRS2* has been ascribed a fundamental role during the progression of cancer [3]. As such, forced *DHRS2* expression significantly reduced tumor growth of ovarian carcinoma and nasopharyngeal carcinoma cells *in vitro* and *in vivo* [4,5]. Also in lung

* Corresponding author. Department of Urology Medical Research Center I, Urological Research Laboratory, Translational UroOncology, Medical Faculty and University Hospital Düsseldorf, Heinrich Heine University, Moorenstraße, 5 40225, Düsseldorf, Germany.
E-mail address: Daniel.Nettersheim@med.uni-duesseldorf.de (D. Nettersheim).
[1] contributed equally.

https://doi.org/10.1016/j.yexcr.2024.114055
Received 23 January 2024; Received in revised form 18 March 2024; Accepted 21 April 2024
Available online 3 May 2024

carcinoma, *DHRS2*-overexpressing cells had a reduced ability of migration, invasion, clonogenicity, and proliferation [6]. Vice versa, low DHRS2 levels were associated with a significantly worse outcome of patients suffering from esophageal squamous cell carcinoma [7]. This study focuses on the current knowledge on the (epigenetic) regulation and function of DHRS2 in urologic malignancies, such as testicular germ cell tumors (GCT), as well as urothelial, prostate, and renal cell carcinoma (UC, PC, RCC).

2. Methods

2.1. Cell culture and standard laboratory techniques

GCT, UC, RCC, and PC cell lines were cultured in the conditions described in Table S1 A and were checked for *Mycoplasma* contamination as well as authenticity (short tandem repeats (STR) profiles). Further standard laboratory techniques, such as cDNA synthesis, qRT-PCR, and western blot analyses have been described elsewhere [8–11]. See Table S1 B-D for detailed information on the utilized drugs, oligos, and antibodies, respectively. Synthesis of the novel HDACi LAK31, KSK64, and MPK409 has been described previously [9].

2.2. Re-analysis of RNA-sequencing data

The RNA-sequencing (RNA-seq) has been performed at the 'Core Facility: Genomics & Transcriptomics' (Heinrich Heine University, Düsseldorf, Germany) as described previously and has been re-analyzed for the purpose of this study (GSE190022, GSE189472) [9,10].

2.3. Assay for transposase-accessible chromatin using sequencing

The assay for transposase-accessible chromatin using sequencing (ATAC-seq) was performed by Active Motif and the data was published elsewhere [9]. The visualization was enabled using the 'Integrated Genome Browser' (https://bioviz.org) [12]. The ATAC-seq data are publicly available via GEO and were re-analyzed in the context of this study (GSE191184).

2.4. Liquid chromatography-mass spectrometry (LC-MS/MS)

Chromatographic separation was performed on a LCMS-8050 triple quadrupole mass spectrometer (Shimadzu Deutschland GmbH, Duisburg, Germany) with a Dual Ion Source and a Nexera X3 Front-End-System (Shimadzu Deutschland GmbH). Chromatographic separation for S1P were performed with a 2 × 60 mm MultoHigh 100 RP18-3 µm column (CS Chromatographie Service, Langerwehe, Germany) at 40 °C. Mobile phases consisted of [A] MeOH and [B] aq. HCO2H (1 % *v/v*) and the following gradient settings were used: [A] increased from 10 % to 100 % over 3 min (B.curve = −2) and returned to 10 % from 8.01 min to 10 min prior next injection. Flow rate was 0.4 ml/min and injection volume of all samples was 10 µl. MS settings were the following: Interface: ESI, nebulizing gas flow: 3 l/min, heating gas flow: 10 l/min, interface temperature: 300 °C, desolvation temperature: 526 °C, DL temperature: 250 °C, heat block temperature: 400 °C, drying gas flow: 10 l/min. Data were collected using multiple reaction monitoring (MRM) and positive ionization $[M+H]^+$ was used for qualitative analysis and quantification. The following MRM transitions were used for quantification: $m/z = 380 \rightarrow 264$ or 82 for S1P ($R_t = 2.67$ min) and $m/z = 366 \rightarrow 250$ for C_{17} S1P ($R_t = 2.55$ min). Standard curves were generated by measuring increased amounts of analytes (10 nM–50 µM S1P; Avanti Polar Lipids Inc., Alabaster, AL, USA) with internal standard (100 nM C_{17} S1P) in MeOH. Chromatographic separation of ceramides were performed with a 2 × 60 mm MultoHigh-C_{18} RP column with 3 µm particle size at 40 °C. Mobile phases consisted of [A] MeOH and [B] aq. HCO_2H (1 % *v/v*) and the following gradient settings were used: [A] increased from 10 % to 100 % over 3 min (B.curve = −2) and returned to 10 % from 8.01 min to 10 min prior next injection. MS settings were the following: Interface: APCI, nebulizing gas flow: 2.4 l/min, heating gas flow: 3 l/min, interface temperature: 300 °C, desolvation temperature: 526 °C, DL temperature: 250 °C, heat block temperature: 400 °C, drying gas flow: 3 l/min. Flow rate was 0.4 ml/min. Standard curves were generated by measuring increased amounts (100 fmol – 50 pmol) of external standards ($Cer_{14:0}$, $Cer_{16:0}$, $Cer_{18:0}$, $Cer_{18:1}$, $Cer_{20:0}$, $Cer_{22:0}$, $Cer_{24:0}$, $Cer_{24:1;}$ Avanti Polar Lipids Inc.) with internal standard (3 pmol $Cer_{15:0;}$ Avanti Polar Lipids Inc.) in methanol. Injection volume of all samples was 10 µl. Data were collected using multiple reaction monitoring (MRM) and positive ionization was used for qualitative analysis and quantification. MRM fragment ions used for quantification were $m/z = 264$ for Cer and $m/z = 284$ for dHCer. Linearity of standard curves and correlation coefficients were obtained by linear regression analysis. Metabolome primary data were analyzed and further processed with LabSolutions 5.99 (Shimadzu Deutschland GmbH) and further processed in Microsoft Excel. 1 pmol S1P/Mio RBC equals 21 µmol/l S1P calculated based on a MCV of 47.5 fl.

2.5. Online analysis tools and statistical analyses

The TCGA ('The Cancer Genome Atlas') cohort was analyzed using 'cBioportal' (https://www.cbioportal.org/) [13], the 'Xena Functional Genomics Explorer' (https://xenabrowser.net/) [14], and the 'Gene Expression Profiling Interactive Analysis' (GEPIA) tool (http://gepia.cancer-pku.cn/) [15]. The 'MusiteDeep' deep-learning framework (https://www.musite.net/) was utilized for the prediction of protein post-translational modification sites [16]. Protein interactions were visualized using the STRING protein interaction algorithm (https://string-db.org/) [17]. Graphical illustrations were designed using 'bioicons' (https://bioicons.com/). Differences between groups were analyzed using a two-tailed Student's t-test and highlighted by asterisks (* = $p < 0.05$).

3. Results

3.1. HDAC inhibition increases chromatin accessibility of the DHRS2 locus eventually enhancing DHRS2 expression

According to the TCGA pan-cancer cohorts, 69 mutations (0.6 % in 10433 evaluated cases) have been noted within the genomic locus of *DHRS2* (NM_005794, *ENST00000250383*), mostly missense single nucleotide polymorphisms (SNP) and deletions (Fig. 1 A; Data S1 A). Further, two fusions were found in the bladder cancer cohorts, namely *DHRS2-GAPDH* and a *DHRS2-IL25* fusion (Fig. 1 A; Data S1 A).

Ten isoforms of the *DHRS2* gene can be transcribed, of which six are protein coding (*ENST00000250383.11*, *ENST00000344777.11*, *ENST00000611765.4*, *ENST00000557535.5*, *ENST00000553600.1*, *ENST00000432832.6*). Using the 'Xena Functional Genomics Explorer', it could be shown that particularly the *DHRS2* isoforms *ENST00000250383.10* and *ENST00000557535.5* were expressed in GCT, UC, PC, RCC as well as their corresponding normal tissues (Fig. 1 B). Based on the GEPIA tool, high levels of *DHRS2* were found in adrenocortical-, breast invasive-, head and neck squamous cell carcinoma, kidney chromophobe, pheochromocytoma and paraganglioma, rectum adenocarcinoma, skin cutaneous melanoma, and thymoma as compared to their respective non-cancerous tissues. Contrariwise, lower *DHRS2* levels were seen in acute myeloid leukemia, ovarian serous cystadenocarcinoma, and GCT in comparison to the corresponding normal tissues, thereby indicating putative different functional roles of DHRS2 during cancer progression (Fig. 1C).

Two alternative *DHRS2* promoter regions were identified, of which one was inducible by the HDACi butyrate in HepG2, THP-1, HT-29, and CaCo-2 cells [18]. HDACi modify the accessibility of the chromatin by inhibiting enzymes responsible for removing acetyl groups, causing an accumulation of histone acetylation and resulting in transcriptional

Fig. 1. Mutational landscape, isoforms, and expression levels of *DHRS2* in tumor tissues. A) Mutational landscape of *DHRS2* in 32 studies including 10.433 samples of the TCGA and visualized using cBioPortal. B) *DHRS2* isoform percentages found in the TCGA TGCT, bladder cancer (BLCA), prostate cancer (PRAD), kidney renal cell carcinoma (KIRC), kidney renal papillary cell carcinoma (KIRP), and kidney chromophobe (KICH) cohorts (purple) in comparison to the respective GTEx normal tissues (blue). Visualized using the 'Xena Functional Genomics Explorer'. qRT-PCR strategy for the detection of various exons depicted as colored arrows. C) *DHRS2* expression levels in several tumor entities (red) compared to respective non-cancerous normal tissues (green) from the TCGA and the GTEx cohorts as evaluated using the GEPIA tool.

hyperactivation [19–21]. Using ATAC-seq of quisinostat-treated 2102 EP embryonal carcinoma (EC) cells, an enhanced accessibility of the genomic *DHRS2* locus was observed (Fig. 2 A). In contrast, DNA methylation seems to play a subordinate role during the HDACi-mediated upregulation of *DHRS2* expression [22]. We further evaluated the *DHRS2* expression in 13 cell lines of various urologic tumor entities (GCT, UC, PC, RCC) treated with the HDACi quisinostat, romidepsin, SAHA/vorinostat, entinostat, LAK31, KSK64, or MPK409 (Fig. 2 B). As such, *DHRS2* levels were enhanced in most of the urologic tumor cell lines (TCam-2, 2102 EP, JAR, GCT72, VM-CUB-1, RT-112, SCaBER, Caki-1, 786-O, ACHN DU-145, PC-3, and LNCaP) treated with the HDACi (Fig. 2 B). Hence, the induction of the *DHRS2* expression can be assumed to be a direct result of a hyperacetylated *DHRS2* locus (Fig. 2 A, B), which has also been previously reported [22,23]. We further re-evaluated RNA-seq data of 2102EP EC cells treated with the HDACi quisinostat or LAK31, as well as VM-CUB-1 (UC), Caki-1 (RCC), and DU-145 (PC) treated with LAK31 with regard to isoform-specific changes in *DHRS2* expression (GSE190022, GSE189472) [9,10]. Treatment with quisinostat or LAK31 resulted in enhanced expression of the protein-coding isoforms *ENST00000553600.1*, *ENST00000557535.5*, *ENST00000250383.11* and *ENST00000344777.11*, as well as the non-protein-coding isoforms *ENST00000556729.1* and *ENST00000556701.5* (Fig. 2 C, D). The highest increase in expression was observed for the *DHRS2 ENST00000250383.11* isoform (Fig. 2 C, D). Using a qRT-PCR-based strategy, we further analyzed the expression of the different *DHRS2* isoforms in 2102EP EC cells treated with either quisinostat, romidepsin or LAK31 (Figs. 1 B, 2 E). In accordance with the RNA-seq data, elevated expression levels of *DHRS2* exon 2/3c, representing the protein-coding isoforms *ENST00000250383.11* and *ENST00000344777.11*, as well as the non-protein-coding isoform *ENST00000556701.5*, were detected in HDACi-treated 2102EP cells (Fig. 2 E). Also on protein levels, elevated DHRS2 levels were observed in quisinostat-treated 2102EP, VM-CUB-1, Caki-1 and PC-3 cells (Fig. 2 F).

3.2. HDACi-induced DHRS2 levels correlate with a pro-apoptotic lipid metabolism

Being located in the cytoplasm, nucleus, and mitochondria, the physiological function of DHRS2 is diverse ranging from the (a) regulation of lipid metabolism by increasing oleic acid and elaidic acid concentrations [2,5], (b) interruption of the choline metabolism [4], (c) (NRF2-dependent) cytoprotection against reactive oxygen species (ROS) [24] to (d) diminished NADP/NADPH ratios [7].

So far, it is not known which role the *DHRS2* deregulation plays in the mechanism of action of HDACi. Hence, we aimed at understanding the causality of elevated DHRS2 levels upon HDACi treatment. The STRING protein interaction algorithm further indicated SHB/D (phosphotyrosine residue binding activity), P3H3 (collagen biosynthesis), TYRP1 (melanin biosynthesis), TTC3 (ubiquitin-dependent protein

Fig. 2. Induction of *DHRS2* expression upon HDAC inhibition in urological malignancies. A) Genomic *DHRS2* locus of 2102EP cells after LAK31 application (red) as compared to the solvent control (blue) as measured by ATAC-seq. B) *DHRS2* expression of urologic tumor cells (TCam-2, 2102EP, JAR, GCT72, VM-CUB-1, RT-112, SCaBER, DU-145, PC-3, LNCaP, Caki-1, 786-O, and ACHN) treated with different HDACi (quisinostat, romidepsin, SAHA/vorinostat, entinostsat, LAK31, KSK64, or MPK409) for 16 h (LD_{50}) in comparison to their solvent control (DMSO) as evaluated by qRT-PCR. *ACTB* and *GAPDH* served as housekeeping genes. C) Detailed re-analysis of RNA-seq data to identify deregulated *DHRS2* isoforms of quisinostat-treated 2102EP cells (16 h) and LAK31-treated 2102EP, VM-CUB-1, Caki-1, and DU-145 cells (24 h) as compared to their solvent control (DMSO). D) Bar graph of the RPKM-values observed in (C). E) qRT-PCR of the different *DHRS2* exons of HDACi (quisinostat, romidepsin, LAK31)-treated 2102EP cells (16 h) as compared to their solvent control (DMSO). *ACTB* and *GAPDH* served as housekeeping genes. F) Western blot analyses indicating DHRS2 protein levels of 2102EP, VM-CUB-1, Caki-1, and PC-3 cells treated for 24 h (LD_{50}) with quisinostat or the solvent control (DMSO). β-Actin served as a loading control. G) STRING interaction analyses of proteins putatively interacting with DHRS2. Two-tailed Student's t-tests were performed to test for significance; *p < 0.05.

catabolic process), DZIP3 (protein polyubiquitination), GMEB1 (glucocorticoid response), HADHA (mitochondrial beta-oxidation of long chain fatty acids), and KYAT3 (tryptophan metabolism) as putatively DHRS2-interacting proteins (Fig. 2 G). Next, we evaluated potential post-translational modifications (PTM) in the DHRS2 protein. According to the MusiteDeep deep-learning platform , histone PTM, such as ubiquitinations (K31, L69), SUMOylation (K147), N6-acetyllysine (K96, K206, K219), or N-linked glycosylation (N186, N229) were predicted to affect DHRS2 (Table 1). However, to our knowledge further validation as well as functional analyses of PTM in DHRS2 are still lacking.

Table 1
Protein PTM site prediction for DHRS2 using the MusiteDeep deep-learning framework (https://www.musite.net/) [16].

PTM	Score	Position	Residue
Methylarginine	0.612	7	R
Ubiquitination	0.658	31	K
Ubiquitination	0.700	69	K
Phosphoserine	0.509	86	S
N6-acetyllysine	0.730	96	K
SUMOylation	0.603	147	K
N-linked glycosylation	0.894	186	N
N6-acetyllysine	0.554	206	K
N6-acetyllysine	0.779	219	K
N-linked glycosylation	0.901	229	N

Being an NADPH-dependent dicarbonylreductase, *DHRS2*-overexpressing KYSE510 cells indicated a decreased NADP/NADPH ratio as compared to the controls. Vice versa, a shRNA-mediated silencing of *DHRS2* in KYSE180 and HKESC1 cells resulted in an enhanced ratio of NADP/NADPH [7]. NADPH is known to maintain reduced glutathione levels, thereby preventing the development of ROS. While an increase in $NADP^+$, NADPH, NAD^+ and NADH has been observed in KRAS-mutant non-small-cell lung cancer cells upon treatment with the HDACi ACY1215 as compared to the control [25], we rather noted marginal changes in all NAD cofactors in quisinostat-treated urologic tumor cells (Fig. 3 A, B; Data S1 B). Further evaluation of the metabolic condition of tumor cells treated with quisinostat revealed commonly enhanced levels of uridine, while inosine levels differed tremendously in a cell line dependent manner. Other factors involved during energy metabolism, such as xantiosine, tryptophan, adenosine, or the ATP/ADP ratio remained rather unchanged (Fig. 3 A, B; Data S1 B).

Previously, enhanced HDACi-mediated upregulation of *DHRS2* expression was linked to increased *CKB* levels, another important factor during cellular energy metabolism [22]. During the *de novo* synthesis of sphingolipids, sphinganine is catalyzed by a ceramide synthase to generate dihydroceramide, which can subsequently be converted to ceramide by a desaturase. Further, ceramide can be converted to (a) ceramide-1-phosphate (C1P) via the ceramide kinase, (b) glucosylceramide by glucosylceramide synthase, (c) sphingomyelin (SM) via the sphingomyelin synthase, or (d) sphingosine by ceramidase. The latter can be further converted to sphingosine-1-phosphate (S1P) by sphingosine kinases (SphK) [26].

To further decipher the potential role of DHRS2-induction upon HDACi treatment, we performed a liquid chromatography-mass spectrometry (LC-MS)-based approach to characterize the lipidomics of HDACi-treated urologic tumor cells (2102EP, VM-CUB-1, Caki-1, PC-3). As such, we observed elevated sphingosine levels in all four quisinostat-treated tumor cells, while reduced levels of S1P were seen (Fig. 3C). Hence, the S1P/sphingosine ratio was significantly diminished upon quisinostat treatment (Fig. 3 D; Data S1 C). This is in accordance with previous descriptions of sphingosines resulting in enhanced apoptosis induction [27]. Evaluating the 'sphingolipid rheostat', a diminished S1P/ceramide ratio was observed in all four quisinostat-treated urologic tumor cells (Fig. 3 D; Data S1 C), thereby representing a pro-apoptotic ceramide generation [28]. These observations were further validated on mRNA level where an induction of the pro-apoptotic factors *APAF1*, *BAK1*, and *NOXA* in correspondence with a downregulation of the anti-apoptotic factors *BCL2* and *BIRC5* was noted in most of the evaluated quisinostat-treated tumor cells in comparison to their respective solvent control (Fig. 3 E). A closer look into the specific SM and ceramide types indicated a rather heterogeneous outcome (Fig. 3C; Data S1 C). Though, the pro-tumoral $SM_{38:1}$ and $SM_{38:2}$ were often diminished in urologic tumor cells upon treatment with quisinostat. While most of the evaluated ceramides were reduced upon quisinostat treatment in 2102EP cells ($Cer_{14:0;16:0;18:0;22:0;24:0;24:1}$), Caki-1 cells indicated elevated ceramide levels (Fig. 3C; Data S1 C), thereby offering a tumor type specific therapeutic approach in combination with HDACi, which could be in part be explained by the elevated DHRS2 levels.

4. Discussion

Functionally, upon translocation of the mitochondrial DHRS2 to the nucleus, DHRS2 is known to inhibit the MDM2-dependent degradation of p53, eventually resulting in p53 stabilization via enhanced S15 phosphorylation, thereby implying a regulatory role of DHRS2 on cell cycle and apoptosis (Fig. 3 F) [29]. As such, a HOXA13-dependent decrease of *DHRS2* expression resulted in increased *MDM2* expression, followed by enhanced p53 degradation [30]. Though, phosphorylation of p53 (S15) remained rather unchanged in GCT cell lines treated with romidepsin or quisinostat [10,31]. Also reduced phosphorylation of Rb (S795) and p38-MAPK (T180/Y182) was noted in *DHRS2*-overexpressing KYSE510 and KYSE30 esophageal squamous cell carcinoma cell lines *in vitro* [7], while AKT phosphorylation (S473) was decreased in *DHRS2*-overexpressing OVCAR3 ovarian carcinoma cells *in vivo* [4]. Moreover, *DHRS2* was shown to be positively regulated by c-Myb in WI-38 fibroblasts [29], FOXR1 in HEK293T cells [32], and LEF1 in JURKAT T-lymphocytes [33], while being negatively regulated by miR-145-3p in TE-8 esophageal squamous cell carcinoma cells [34], polyP kinase expression in HEK293T [35], and HOXA13 in gastric cancer (Fig. 3 F) [30]. With regard to *DHRS2* regulation via changes in the epigenetic machinery, it was shown in RCC that a knockdown of the histone methyltransferase *SUV420H2* resulted in H4K20 tri-methylation within the *DHRS2* promotor region, eventually resulting in increased *DHRS2* expression [36]. Further studies, including our own (here presented) work, observed significantly enhanced *DHRS2*/DHRS2 levels upon treatment with various HDACi, such as SAHA/vorinostat, valproic acid, entinostat, trichostatin A (TSA), MS-275, CRA-024781, LBH589, apacidin, romidepsin, quisinostat, LAK31, KSK64, MPK409, and panobinostat (Table 2) [9,10,22,31,37–43]. Of note, the *DHRS2* paralogue *DHRS4* does not seem to be implicated in the HDACi-mediated response cascade [22]. Previous studies have shown that HDACi-induced *DHRS2* expression levels correlated with enhanced H3ac [22] as well as H3K27ac [23]. The here presented study further confirmed an enhanced accessibility of the genomic *DHRS2* locus upon HDACi treatment. Currently, the HDACi SAHA/vorinostat (pan), romidepsin (HDAC1/2), belinostat (pan), panobinostat (pan), and chidamide (HDAC1/2/3/10) have been approved for clinical use [44], while ongoing clinical trials are investigating the safety, tolerability, and efficacy of the 'second-generation' HDACi quisinostat with first results showing high efficacy and good tolerability [45–48]. Despite their clinical use since 15 years and even though several multifactorial HDACi resistance mechanisms have been described *in vitro*, only few cases describe resistance mechanisms in the clinics [44,49]. Nevertheless, with regard to the putative development of HDACi resistance, a shRNA-mediated knockdown of *DHRS2* expression was concomitant with a diminished efficacy of SAHA treatment *in vivo* [42].

Besides *DHRS2*, other HDACi-dependent key factors have been previously identified, such as *RHOB*, *GADD45B*, *CDKN1A*, *ATF3*, *DUSP1*, *FOS*, and *ID2*, which are known to regulate stress response, apoptosis induction, and cell cycle distribution [9,22,31]. Concomitantly, lack of *DHRS2* in TCam-2 cells did not only have marginal effects on transcriptome-wide changes as compared to their parental controls, it also did not have an influence on the expression of HDACi-induced key players upon treatment with romidepsin [22], thereby suggesting DHRS2 to act rather independently of these stress-related factors during the HDACi downstream signaling.

This study further aimed at understanding the functional role of HDACi-mediated induction of DHRS2 levels. Hence, the energy- and lipid metabolisms were investigated pan-urologically in tumor cells treated with the HDACi quisinostat. While NAD cofactors in quisinostat-treated urologic tumor cells remained rather unchanged, the NADPH oxidase (Nox) protein family has been ascribed as are a major regulator

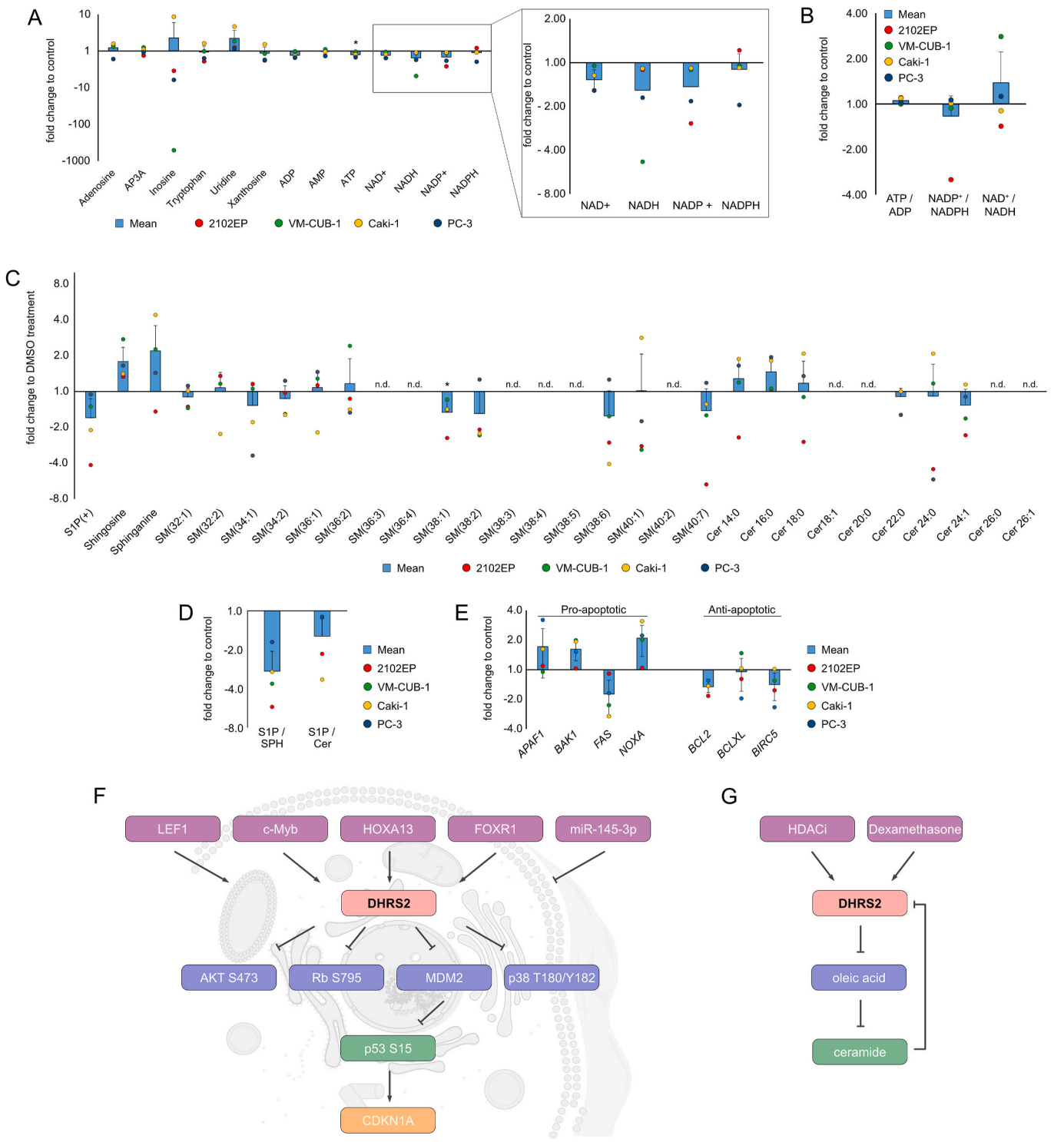

Fig. 3. Energy metabolism and lipidomics of HDACi-treated urologic tumor cells. A) Evaluation of the energy metabolism of urologic tumor cells (2102EP, VM-CUB-1, Caki-1, PC-3) treated with quisinostat for 24 h (LD_{50}) as compared to the solvent control (DMSO). B) Relative ratio of ATP/ADP, $NADP^+$/NADPH, and NAD^+/NADH in quisinostat-treated urologic tumor cells (2102EP, VM-CUB-1, Caki-1, PC-3) as compared to the solvent control. C) Evaluation of the lipid metabolism in 2102EP, VM-CUB-1, Caki-1 and PC-3 cells treated with quisinostat or DMSO as evaluated by means of LC-MS. D) Calculated S1P/SPH and S1P/ceramide ratios based on the findings observed in (C). E) mRNA levels of *APAF1*, *BAK1*, *FAS*, *NOXA*, *BCL2*, *BCLXL*, and *BIRC5* in urologic tumor cells (2102EP, VM-CUB-1, Caki-1, PC-3) treated with quisinostat for 24 h (LD_{50}) as compared to the solvent control (DMSO). *ACTB* and *GAPDH* served as housekeeping genes. F) Graphical summary of the functional role of DHRS2. G) Illustration of the therapeutic options involving DHRS2. Two-tailed Student's t-tests were performed to test for significance; *$p < 0.05$.

of ROS production. As such, decreased levels of Nox enzymes were noted in pulmonary arterial hypertension, human atherosclerosis, or HUVEC cells treated with the HDACi [50,51]. However, our transcriptome-wide analyses of romidepsin-, quisinostat-, givinostat-, SAHA- or LAK31-treated urologic tumor cells could not confirm these observations (GSE70120, GSE190022, GSE189472) [9,10,31,41].

Regarding the evaluation of lipidomics, enhanced ceramide and sphingosine levels have been associated with diminished tumor growth

Table 2
Studies showing enhanced DHRS2-levels upon HDACi-treatment.

Tumor entity	Cell lines	HDACi	Model	Reference
Germ cell tumor Urothelial carcinoma Renal cell carcinoma Prostate carcinoma	TCam-2 2102EP JAR GCT72 VM-CUB-1 Caki-1 DU-145	LAK31 KSK64 MPK409	*in vitro*	[9]
Germ cell tumor	TCam-2 2102EP JAR GCT72	Quistinostat	*in vitro*	[10]
Germ cell tumor	TCam-2 2102EP JAR	Romidepsin	*in vitro*	[22]
Germ cell tumor Fibroblasts Sertoli cells	TCam-2 2102EP/–R NCCIT/–R NT2/D1/–R JAR JEG-3 MPAF ARZ FS1	Romidepsin	*in vitro*	[31]
Glioblastoma Pancreas carcinoma	T98G PANC-1	Panobinostat	*In vitro*	[37]
Urothelial carcinoma	T24	SAHA/ Vorinostat Trichostatin A MS-275	*in vitro*	[38]
Colorectal carcinoma	HCT116 HT29	SAHA/ Vorinostat	*in vitro*	[39]
Colorectal carcinoma	HCT116	CRA-024781	*in vivo*	[40]
Urothelial carcinoma	UM-UC-3 VM-CUB-1	SAHA/ Vorinostat Romidepsin	*in vitro*	[41]
Ovarian carcinoma	ES2 A2780	SAHA/ Vorinostat Apacidin Trichostatin A	*in vitro*	[42]
Leukemia	CMK HEL K-562 NB-4 HL-60	Valproic acid	*in vitro* *ex vivo*	[43]

and apoptosis induction, while S1P and C1P were correlated with elevated proliferation [26,27]. However, even though $C_{12\text{-}26}$-ceramide were shown to result in growth inhibition, C_{16}-ceramide was described to be involved during tumor proliferation in head and neck squamous cell carcinoma [52,53].

In this study, we demonstrated diminished S1P/sphingosine as well as S1P/ceramide (sphingolipid rheostat) levels (Fig. 3 D, Data S1 C), thereby indicating the promotion of a pro-apoptotic state [27,28]. Interestingly, Xu et al. observed that the administration of oleic acid, which was previously shown to be negatively regulated by DHRS2 [5], significantly diminished ceramide levels in hepatocytes [54]. Hence, HDACi-mediated enhanced DHRS2 activity could diminish oleic acid levels, thereby resulting in induced generation of ceramides. Interestingly, Cao et al. observed, besides several histone-regulating genes, *DHRS2* to be among the most prominently downregulated genes upon treatment with exogenous dihydroceramide (dhC16-Cer) in lymphoma cells, thereby indicating a putative negative feedback loop of *DHRS2* expression [55] (Fig. 3 G).

Previuosly, we could show that besides *DHRS2*, several other stress-related genes, such as *GADD45B*, *DUSP1*, *FOS*, *ID2*, *RHOB*, and *ATF3*, were upregulated upon HDACi treatment in GCT cells [9,22,31], all of which are also known to be glucocorticoid response genes [22]. Hence, in our previous investigation, a combined therapeutic approach using the glucocorticoid steroid dexamethasone for 8 days followed by the addition of the HDACi romidepsin for 16 h not only significantly enhanced the expression of *GADD45B*, *DUSP1*, and *DHRS2* as compared to the HDACi treatment alone, but also resulted in decreased cell viability in GCT cells (TCam-2, 2102EP, JAR) in comparison to the single HDACi treatment [22].

The role of DHRS2 as a therapeutic target still needs to be further elucidated. While low *DHRS2* levels were seen in tamoxifen-resistant MCF-7 breast carcinoma cells and 5-fluorouracil-treated in HCT116 colon carcinoma cells [56,57], downregulation of *DHRS2* sensitized oxaliplatin-resistant HCT116 colon carcinoma cells by downregulating *ERCC1* in a p53-dependent manner [58]. Moreover, since DHRS2 was previously identified as a WNT4-associated protein [59] and LEF1 was described as a positive regulator of *DHRS2* expression [33], modulating the WNT/β-catenin signaling cascade could offer a promising targetable pathway in combination with HDACi treatment (Fig. 3 F).

5. Conclusion

Emphasizing on urologic malignancies, such as GCT, UC, RCC and PC, this study observed that enhanced DHRS2 levels upon HDACi treatment correlated with an increased chromatin accessibility of the *DHRS2* locus, thereby enabling its presence as an indication of a successful HDACi treatment. The identification of a pro-apoptotic lipid metabolism in HDACi-treated urologic tumor cells offers further therapeutic strategies for a combined treatment resulting in the reprogramming of the fatty acid metabolism [60]. Further evaluation of the literature gives rise to the hypothesis that enhanced DHRS2 levels, either through activation of the WNT/β-catenin signaling pathway or treatment with HDACi or glucocorticoid steroids (e.g. dexamethasone), as well as its stabilization through the application of oleic acid (Fig. 3 F, G) could have an anti-tumor effect in urologic malignancies.

Ethics approval and consent to participate

The ethics committee of the Heinrich Heine University Düsseldorf raised no concerns on utilizing cell lines for *in vitro* experiments (vote 2018-178 to D. N.).

Consent for publication

All authors are aware of this article and agreed on publication.

Funding

D. Nettersheim was kindly supported by the ‘Brigitte & Dr. Konstanze Wegener-Stiftung‘ (Projekt #36, Projekt #84). M. A. Skowron was supported by the ’Research Committee of the Faculty of Medicine of the Heinrich Heine University Düsseldorf’. B. Levkau was supported by the ’German Research Foundation’ (LE 940/7-1 and TRR259, project B10).

CRediT authorship contribution statement

Melanie R. Müller: Writing – review & editing, Writing – original draft, Visualization, Validation, Investigation, Formal analysis. **Aaron Burmeister:** Writing – review & editing, Writing – original draft, Visualization, Validation, Investigation, Formal analysis. **Margaretha A. Skowron:** Writing – review & editing, Writing – original draft, Visualization, Validation, Investigation, Formal analysis. **Alexa Stephan:** Investigation, Formal analysis. **Christian Söhngen:** Investigation, Formal analysis. **Philipp Wollnitzke:** Investigation, Formal analysis. **Patrick Petzsch:** Visualization, Software, Formal analysis, Data curation. **Leandro A. Alves Avelar:** Resources. **Thomas Kurz:** Resources. **Karl Köhrer:** Writing – review & editing, Software, Methodology, Formal analysis, Data curation, Resources. **Bodo Levkau:** Writing – review & editing, Visualization, Software, Resources,

Methodology, Formal analysis, Data curation. **Daniel Nettersheim:** Writing – review & editing, Writing – original draft, Visualization, Supervision, Resources, Project administration, Methodology, Investigation, Funding acquisition, Formal analysis, Conceptualization.

Declaration of competing interest

The authors declare that they have no known competing financial interests or personal relationships that could have appeared to influence the work reported in this paper.

Data availability

Data will be made available on request.

Acknowledgements

We kindly thank Anna Pehlke for excellent technical assistance. We would like to thank Dr. Christoph Oing, Dr. Thomas Müller, Dr Janet Shipley, Prof. Dr. Bernd Schmitz-Dräger, Prof. Dr. Margaret Knowles and PD Dr. med Isabella Syring-Schmandke for providing cell lines and healthy control cells (see Table S1 A for affiliations and provided cell lines). We further thank Prof. Dr. Thomas Kurz and Dr. Leandro A. Alves Avelar for providing the HDACi LAK31, KSK64, and MPK409 (Table S1 B).

List of abbreviations

C1P	Ceramide-1-phosphate
DHRS2	Dehydrogenase/reductase member 2
EC	Embryonal carcinoma
HDACi	Histone deacetylase inhibitor
GCT	Germ cell tumor
LC-MS	Liquid chromatography-mass spectrometry
MRM	Multiple reaction monitoring
NAD	Nicotinamide adenine dinucleotide
NADP	Nicotinamide adenine dinucleotide phosphate
PC	Prostate cancer
PTM	Post-translational modification
RCC	Renal cell carcinoma
ROS	Reactive oxygen species
RPKM	Reads per kilobase million
SDR	Short-chain dehydrogenase/reductase
SM	Sphingomyelin
SNP	Single nucleotide polymorphisms
S1P	Sphingosine-1-phosphate
SphK	Sphingosine kinases (SphK)
TCGA	The Cancer Genome Atlas
TSA	Trichostatin A
UC	Urothelial carcinoma

Appendix A. Supplementary data

Supplementary data to this article can be found online at https://doi.org/10.1016/j.yexcr.2024.114055.

References

[1] G. Donadel, C. Garzelli, R. Frank, F. Gabrielli, Identification of a novel nuclear protein synthesized in growth-arrested human hepatoblastoma HepG2 cells, Eur. J. Biochem. 195 (1991) 723–729.
[2] Z. Li, H. Liu, A. Bode, X. Luo, Emerging roles of dehydrogenase/reductase member 2 (DHRS2) in the pathology of disease, Eur. J. Pharmacol. 898 (2021).
[3] S. Pellegrini, S. Censini, S. Guidotti, P. Iacopetti, M. Rocchi, M. Bianchi, et al., A human short-chain dehydrogenase/reductase gene: Structure, chromosomal localization, tissue expression and subcellular localization of its product, Biochim. Biophys. Acta Gene Struct. Expr. 1574 (2002) 215–222.
[4] Z. Li, Y. Tan, X. Li, J. Quan, A.M. Bode, Y. Cao, et al., DHRS2 inhibits cell growth and metastasis in ovarian cancer by downregulation of CHKα to disrupt choline metabolism, Cell Death Dis. 13 (2022).
[5] X. Luo, N. Li, X. Zhao, C. Liao, R. Ye, C. Cheng, et al., DHRS2 mediates cell growth inhibition induced by Trichothecin in nasopharyngeal carcinoma, J. Exp. Clin. Cancer Res. 38 (2019).
[6] X. Yang, L. Ling, C. Li, T. Hu, C. Zhou, J. Chen, et al., STAMBPL1 promotes the progression of lung adenocarcinoma by inhibiting DHRS2 expression, Transl Oncol 35 (2023).
[7] Y. Zhou, L. Wang, X. Ban, T. Zeng, Y. Zhu, M. Li, et al., DHRS2 inhibits cell growth and motility in esophageal squamous cell carcinoma, Oncogene 37 (2018 378. 2017) 1086–1094.
[8] M.A. Skowron, T.K. Becker, L. Kurz, S. Jostes, F. Bremmer, F. Fronhoffs, et al., The signal transducer CD24 suppresses the germ cell program and promotes an ectodermal rather than mesodermal cell fate in embryonal carcinomas, Mol. Oncol. 16 (2021) 982–1008.
[9] A. Burmeister, A. Stephan, L.A. Alves Avelar, M.R. Müller, A. Seiwert, S. Höfmann, et al., Establishment and evaluation of a dual HDAC/BET inhibitor as a therapeutic option for germ cell tumors and other urological malignancies, Mol Cancer Ther 21 (2022) 1674–1688.
[10] M.R. Müller, A. Burmeister, M.A. Skowron, A. Stephan, F. Bremmer, G.A. Wakileh, et al., Therapeutical interference with the epigenetic landscape of germ cell tumors: a comparative drug study and new mechanistical insights, Clin Epigenetics 14 (2022) 5.
[11] G.A. Wakileh, P. Bierholz, M. Kotthoff, M.A. Skowron, F. Bremmer, A. Stephan, et al., Molecular characterization of the CXCR4/CXCR7 axis in germ cell tumors and its targetability using nanobody-drug-conjugates, Exp. Hematol. Oncol. 12 (2023) 96.
[12] N.H. Freese, D.C. Norris, A.E. Loraine, Integrated genome browser: visual analytics platform for genomics, Bioinformatics 32 (2016) 2089–2095.
[13] E. Cerami, J. Gao, U. Dogrusoz, B.E. Gross, S.O. Sumer, B.A. Aksoy, et al., The cBio Cancer Genomics Portal: an open platform for exploring multidimensional cancer genomics data, Cancer Discov. 2 (2012) 401–404.
[14] M. Goldman, B. Craft, A. Brooks, J. Zhu, D. Haussler, Visualizing and interpreting cancer genomics data via the Xena platform, Nat. Biotechnol. 38 (2020) 675–678.
[15] Z. Tang, C. Li, B. Kang, G. Gao, C. Li, Z. Zhang, GEPIA: a web server for cancer and normal gene expression profiling and interactive analyses, Nucleic Acids Res. 45 (2017) W98–W102.
[16] D. Wang, D. Liu, J. Yuchi, F. He, Y. Jiang, S. Cai, et al., MusiteDeep: a deep-learning based webserver for protein post-translational modification site prediction and visualization, Nucleic Acids Res. 48 (2020) W140–W146.
[17] D. Szklarczyk, A.L. Gable, D. Lyon, A. Junge, S. Wyder, J. Huerta-Cepas, et al., STRING v11: protein-protein association networks with increased coverage, supporting functional discovery in genome-wide experimental datasets, Nucleic Acids Res. 47 (2019) D607–D613.
[18] S. Heinz, S.W. Krause, F. Gabrielli, H.M. Wagner, R. Andreesen, M. Rehli, Genomic organization of the human gene HEP27: alternative promoter usage in HepG2 cells and monocyte-derived dendritic cells, Genomics 79 (2002) 608–615.
[19] A.C. West, R.W. Johnstone, New and emerging HDAC inhibitors for cancer treatment, J. Clin. Invest. 124 (2014) 30–39.
[20] Y. Li, E. Seto, HDACs and HDAC inhibitors in cancer development and therapy, Cold Spring Harb Perspect Med. 6 (2016) a026831.
[21] S.Y. Park, J.S. Kim, A short guide to histone deacetylases including recent progress on class II enzymes, Exp. Mol. Med. 522 (52) (2020) 204–212, 2020.
[22] D. Nettersheim, D. Berger, S. Jostes, M. Skowron, H. Schorle, Deciphering the molecular effects of romidepsin on germ cell tumours: DHRS2 is involved in cell cycle arrest but not apoptosis or induction of romidepsin effectors, J. Cell Mol. Med. 23 (2019) 670–679.
[23] A. Barrett, M.R. Shingare, A. Rechtsteiner, T.U. Wijeratne, K.M. Rodriguez, S. M. Rubin, et al., HDAC activity is dispensable for repression of cell-cycle genes by DREAM and E2F:RB complexes, bioRxiv Prepr Serv Biol. (2023).
[24] D. Crean, L. Felice, C.T. Taylor, H. Rabb, P. Jennings, M.O. Leonard, Glucose reintroduction triggers the activation of Nrf2 during experimental ischemia reperfusion, Mol. Cell. Biochem. 366 (2012) 231–238.
[25] H. Zhang, C.S. Nabel, D. Li, R. O'Connor, C.R. Crosby, S.M. Chang, et al., Histone deacetylase 6 inhibition exploits selective metabolic vulnerabilities in LKB1 mutant, KRAS driven NSCLC, J. Thorac. Oncol. 18 (2023) 882–895.
[26] N.C. Hait, A. Maiti, The role of sphingosine-1-phosphate and ceramide-1-phosphate in inflammation and cancer, Mediat. Inflamm. (2017 (2017) 4806541.
[27] O. Companioni, C. Mir, Y. Garcia-Mayea, M.E. Lleonart, Targeting sphingolipids for cancer therapy, Front. Oncol. 11 (2021).
[28] J. Newton, S. Lima, M. Maceyka, S. Spiegel, Revisiting the sphingolipid rheostat: evolving concepts in cancer therapy, Exp. Cell Res. 333 (2015) 195–200.
[29] C. Deisenroth, A.R. Thorner, T. Enomoto, C.M. Perou, Y. Zhang, Mitochondrial Hep27 is a c-Myb target gene that inhibits Mdm2 and stabilizes p53, Mol. Cell Biol. 30 (2010) 3981–3993.
[30] Y. Han, C. Song, J. Wang, H. Tang, Z. Peng, S. Lu, HOXA13 contributes to gastric carcinogenesis through DHRS2 interacting with MDM2 and confers 5-FU resistance by a p53-dependent pathway, Mol. Carcinog. 57 (2018) 722–734.
[31] D. Nettersheim, S. Jostes, M. Fabry, F. Honecker, V. Schumacher, J. Kirfel, et al., A signaling cascade including ARID1A, GADD45B and DUSP1 induces apoptosis and affects the cell cycle of germ cell cancers after romidepsin treatment, Oncotarget 7 (2016) 74931–74946.
[32] A. Mota, H.K. Waxman, R. Hong, G.D. Lagani, S.Y. Niu, F.L. Bertherat, et al., FOXR1 regulates stress response pathways and is necessary for proper brain development, PLoS Genet. 17 (2021).

[33] S.S. Ekmekci, Z. Emrence, N. Abacı, M. Sarıman, B. Salman, C.G. Ekmekci, et al., LEF1 induces DHRS2 gene expression in human acute leukemia jurkat T-cells, Turkish J Haematol Off J Turkish Soc Haematol 37 (2020) 226–233.
[34] M. Shimonosono, T. Idichi, N. Seki, Y. Yamada, T. Arai, T. Arigami, et al., Molecular pathogenesis of esophageal squamous cell carcinoma: identification of the antitumor effects of miR-145-3p on gene regulation, Int. J. Oncol. 54 (2019) 673–688.
[35] E. Bondy-Chorney, I. Abramchuk, R. Nasser, C. Holinier, A. Denoncourt, K. Baijal, et al., A broad response to intracellular long-chain polyphosphate in human cells, Cell Rep. 33 (2020).
[36] T.Y. Ryu, J. Lee, Y. Kang, M.Y. Son, D.S. Kim, Y su Lee, et al., Epigenetic regulation of DHRS2 by SUV420H2 inhibits cell apoptosis in renal cell carcinoma, Biochem. Biophys. Res. Commun. 663 (2023) 41–46.
[37] R.M. Duncan, L. Reyes, K. Moats, R.M. Robinson, S.A. Murphy, B. Kaur, et al., ATF3 coordinates antitumor synergy between epigenetic drugs and protein disulfide isomerase inhibitors, Cancer Res. 80 (2020) 3279–3291.
[38] K.B. Glaser, M.J. Staver, J.F. Waring, J. Stender, R.G. Ulrich, S.K. Davidsen, Gene Expression Profiling of Multiple Histone Deacetylase (HDAC) Inhibitors: Defining a Common Gene Set Produced by HDAC Inhibition in T24 and MDA Carcinoma Cell Lines. Mol Cancer Ther. 2 (2003)151-63.
[39] M.J. Labonte, P.M. Wilson, W. Fazzone, S. Groshen, H.J. Lenz, R.D. Ladner, DNA microarray profiling of genes differentially regulated by the histone deacetylase inhibitors vorinostat and LBH589 in colon cancer cell lines, BMC Med. Genom. 2 (2009) 67.
[40] J.J. Buggy, Z.A. Cao, K.E. Bass, E. Verner, S. Balasubramanian, L. Liu, et al., CRA-024781: a novel synthetic inhibitor of histone deacetylase enzymes with antitumor activity in vitro and in vivo, Mol Cancer Ther 5 (2006) 1309–1317.
[41] M. Pinkerneil, M.J. Hoffmann, R. Deenen, K. Köhrer, T. Arent, W.A. Schulz, et al., Inhibition of class I histone deacetylases 1 and 2 promotes urothelial carcinoma cell death by various mechanisms, Mol Cancer Ther 15 (2016) 299–312.
[42] Y. Han, Z. Wang, S. Sun, Z. Zhang, J. Liu, X. Jin, et al., Decreased DHRS2 expression is associated with HDACi resistance and poor prognosis in ovarian cancer, Epigenetics 15 (2020) 122–133.
[43] F.G. Rücker, K.M. Lang, M. Fütterer, V. Komarica, M. Schmid, H. Döhner, et al., Molecular dissection of valproic acid effects in acute myeloid leukemia identifies predictive networks, Epigenetics 11 (2016) 517–525.
[44] F. Fischer, L.A. Alves Avelar, A short overview of resistance to approved histone deacetylase inhibitors, Future Med. Chem. 13 (2021) 1153–1155.
[45] J. Arts, P. King, A. Mariën, W. Floren, A. Beliën, L. Janssen, et al., JNJ-26481585, a novel "second-generation" oral histone deacetylase inhibitor, shows broad-spectrum preclinical antitumoral activity, Clin. Cancer Res. 15 (2009) 6841–6851.
[46] B. Venugopal, R. Baird, R.S. Kristeleit, R. Plummer, R. Cowan, A. Stewart, et al., A phase i study of quisinostat (JNJ-26481585), an oral hydroxamate histone deacetylase inhibitor with evidence of target modulation and antitumor activity, in patients with advanced solid tumors, Clin. Cancer Res. 19 (2013) 4262–4272.
[47] S. Tjulandin, M. Fedyanin, V.I. Vladimirov, V. Kostorov, A.S. Lisyanskaya, L. Krikunova, et al., A multicenter phase II study of the efficacy and safety of quisinostat (an HDAC inhibitor) in combination with paclitaxel and carboplatin chemotherapy (CT) in patients (pts) with recurrent platinum resistant high grade serous epithelial ovarian, primarily, J. Clin. Oncol. 35 (2017) 5541, 5541.
[48] F. Child, P.L. Ortiz-Romero, R. Alvarez, M. Bagot, R. Stadler, M. Weichenthal, et al., Phase II multicentre trial of oral quisinostat, a histone deacetylase inhibitor, in patients with previously treated stage IB–IVA mycosis fungoides/Sézary syndrome, Br. J. Dermatol. 175 (2016) 80–88.
[49] J.H. Lee, M.L. Choy, P.A. Marks, Mechanisms of resistance to histone deacetylase inhibitors, Adv. Cancer Res. 116 (2012) 39–86.
[50] N.Y. Hakami, G.J. Dusting, H.M. Peshavariya, Trichostatin A, a histone deacetylase inhibitor suppresses NADPH oxidase 4-derived redox signalling and angiogenesis, J. Cell Mol. Med. 20 (2016) 1932–1944.
[51] F. Chen, X. Li, E. Aquadro, S. Haigh, J. Zhou, D.W. Stepp, et al., Inhibition of histone deacetylase reduces transcription of NADPH oxidases and ROS production and ameliorates pulmonary arterial hypertension, Free Radic. Biol. Med. 99 (2016) 167–178.
[52] S. Ponnusamy, M. Meyers-Needham, C.E. Senkal, S.A. Saddoughi, D. Sentelle, S. P. Selvam, et al., Sphingolipids and cancer: ceramide and sphingosine-1-phosphate in the regulation of cell death and drug resistance, Future Oncol. 6 (2010) 1603–1624.
[53] S. Schiffmann, J. Sandner, K. Birod, I. Wobst, C. Angioni, E. Ruckhäberle, et al., Ceramide synthases and ceramide levels are increased in breast cancer tissue, Carcinogenesis 30 (2009) 745–752.
[54] C. Xu, D. Song, A.L. Holck, Y. Zhou, R. Liu, Identifying lipid metabolites influenced by oleic acid administration using high-performance liquid chromatography-mass spectrometry-based lipidomics, ACS Omega 5 (2020) 11314–11323.
[55] Y. Cao, J. Qiao, Z. Lin, J. Zabaleta, L. Dai, Z. Qin, Up-regulation of tumor suppressor genes by exogenous dhC16-Cer contributes to its anti-cancer activity in primary effusion lymphoma, Oncotarget 8 (2017) 15220–15229.
[56] U. Ozer, K.W. Barbour, S.A. Clinton, F.G. Berger, Oxidative stress and response to thymidylate synthase-targeted antimetabolites, Mol. Pharmacol. 88 (2015) 970–981.
[57] X. Men, J. Ma, T. Wu, J. Pu, S. Wen, J. Shen, et al., Transcriptome profiling identified differentially expressed genes and pathways associated with tamoxifen resistance in human breast cancer, Oncotarget 9 (2017) 4074–4089.
[58] J.M. Li, G.M. Jiang, L. Zhao, F. Yang, W.Q. Yuan, Y.Q. Luo, et al., Dehydrogenase/reductase SDR family member 2 silencing sensitizes an oxaliplatin-resistant cell line to oxaliplatin by inhibiting excision repair cross-complementing group 1 protein expression, Oncol. Rep. 42 (2019) 1725–1734.
[59] J.L. Sottnik, M.T. Shackleford, S.K. Robinson, F.R. Villagomez, S. Bahnassy, S. Oesterreich, et al., WNT4 regulates cellular metabolism via intracellular activity at the mitochondria in breast and gynecologic cancers, Cancer Res Commun 4 (2024) 134–151.
[60] N. Koundouros, G. Poulogiannis, Reprogramming of fatty acid metabolism in cancer, Br. J. Cancer 122 (2020) 4–22.